Acta Oceanol. Sin., 2019, Vol. 38, No. 5, P. 109–117
https://doi.org/10.1007/s13131-019-1357-y
http://www.hyxb.org.cn
E-mail: hyxbe@263.net

Effects of igneous bodies on modification of modern slope morphology: Insights from the continental slope offshore Dongsha Islands, South China Sea

Chao Liang[1, 2], Xinong Xie[1, 2*], Hua Wang[2, 3], Guangjian Zhong[4], Entao Liu[1, 2], Ming Sun[4], Hai Yi[4], Chunyu Qin[3], Haiyang Cao[5], Jie He[3], Yanpu Zhao[3]

[1] College of Marine Science and Technology, China University of Geosciences, Wuhan 430074, China

[2] Key Laboratory of Tectonics and Petroleum Resources of Ministry of Education, China University of Geosciences, Wuhan 430074, China

[3] Faculty of Earth Resources, China University of Geosciences, Wuhan 430074, China

[4] Guangzhou Marine Geological Survey, China Geological Survey, Guangzhou 510760, China

[5] Institute of Sedimentary Geology, Chengdu University of Technology, Chengdu 610059, China

Received 24 November 2017; accepted 10 February 2018

Abstract

A statistical analysis for the morphological parameters extracted from numerous seismic profiles, and a high-resolution seismic study of the southeastern slope of the Dongsha Islands (South China Sea) with water depth between approximately 500 and 3 100 m, has revealed the variation of morphological features due to the intrusion of igneous bodies and associated sedimentary processes. Three types of the continental slope are distinguished: (1) a rough and steep slope with multiple igneous bodies (Type 1), (2) a relatively smooth and gentle slope with the single igneous body (Type 2), and (3) a smooth and gentle slope without igneous bodies (Type 3). These igneous bodies, formed in the post-seafloor spreading of the South China Sea, are often characterized by high positive seismic amplitudes, and chaotic reflections with complex shapes. The igneous bodies in Type 1 separated the slope into two or more upper sub-sags and a lower main-sag, in which the sub-sags and main-sag could be filled with sediments transported by alongslope bottom currents at the same time. Whereas, the igneous body in Type 2 just separated the slope into an upper sub-sag and a lower main-sag, in which the sediments could be transported into the lower main-sag only after the upper sub-sag has been filled up. Type 3 represents a normal slope with common clinoform progradation. The modern slope morphologies in the study area are the results of adjustments of the continental slope due to the intrusion of igneous bodies and associated sedimentary processes. The distinctions among three types of modern slope morphologies indicate different depositional conditions and adjustments of slope morphologies.

Key words: igneous bodies, modern slope morphology, Dongsha Islands, South China Sea

Citation: Liang Chao, Xie Xinong, Wang Hua, Zhong Guangjian, Liu Entao, Sun Ming, Yi Hai, Qin Chunyu, Cao Haiyang, He Jie, Zhao Yanpu. 2019. Effects of igneous bodies on modification of modern slope morphology: Insights from the continental slope offshore Dongsha Islands, South China Sea. Acta Oceanologica Sinica, 38(5): 109–117, doi: 10.1007/s13131-019-1357-y

1 Introduction

Modern continental slope morphology is the product of variously complex geologic processes that might be constructional or destructional over millions of years (Brothers et al., 2013), whereas many present continental slope morphologies are mainly reflective of recent and ongoing geological processes (O'Grady et al., 2000). Moreover, a series of crucial factors have been proposed to explain the variation of modern continental slope morphology, such as sediment supply (Kenyon and Turcotte, 1985; Goff, 2001; O'Grady et al., 2000), sediment grain size (Adams et al., 1998), sedimentary texture (Schlager and Camber, 1986), sedimentary transport mechanisms (Cacchione et al., 2002), sediment over loading and tectonic deformation (Del Bianco et al., 2015), bottom currents (García et al., 2009; Sayago-Gil et al., 2010; Chen et al., 2014), the presence of mobile substrates (Pratson and Haxby, 1996), and so forth. However, rare attention has been paid to the relationship between igneous bodies and modern slope morphology. In addition, the accurate effects of igneous bodies on modification of modern slope morphology also remains ambiguous.

An enormous body of evidence from seismic and drilling data document that a spot of small-scale late Oligocene–middle Miocene volcanism occurred sporadically on the northern South China Sea margin (Li and Rao, 1994), however, the Neogene magma activities along the lower slope of the northern South China Sea were fierce (Lüdmann and Wong, 1999; Song et al., 2017). Igneous bodies formed by magma emplacement could also be recognized on the seismic profiles in our study area,

Foundation item: The National Natural Science Foundation of China under contract Nos 91528301, 41702121, 41606074 and 41702114; the National Science and Technology Major Project under contract No. 2017ZX05026-005-002; the Survey of Oil and Gas Resources in the Northern South China Sea and Taiwan Strait under contract No. DD20160154.
*Corresponding author, E-mail: xnxie@cug.edu.cn

where represents an unique opportunity to examine the relationship between igneous bodies and modern slope morphology.

In this paper, we describe and analyze modern slope morphology formed by igneous bodies and associated sedimentary processes, as well as document the effects of igneous bodies on modification of modern slope morphology in detail. Finally, conceptual models are presented and discussed.

2 Regional setting

The South China Sea (SCS), one of the biggest margin sea of the West Pacific, lies at the intersections of the Eurasian Plate, Philippine Sea Plate and Indo-Australian Plate (Zhang and Zhong, 1996; Cheng et al., 2012). As the result of Cenozoic continental margin rifting, the South China Sea has experienced a complete Wilson Cycle (Song et al., 2017), which drifted to its present position in the Middle Miocene, with a subsequent seafloor spreading in its central part (Taylor and Hayes, 1983). The northern margin of SCS is a portion of the South China Block, which is floored with continental crust (Yao et al., 2004). The Dongsha Islands are located in the central part of the northern margin of the SCS, and the study area (black rectangle in Fig. 1a) is situated on the southeast of Dongsha Islands between 18.37° and 20.92°N, and 116.52° and 118.23°E, with the water depth of approximately 500–3 100 m. The continental slope in the study area tilts from northwest to southeast (Fig. 1b).

Consistent with the tectonic evolution of the northern margin of the SCS, the research area was affected by multiple tectonic events during the Cenozoic (Taylor and Hayes, 1983), for instance, the rifting of the South China Sea Basin and tectonic escape of the Indochina Block (Zhang and Zhong, 1996), and so on. However, the most prominent tectonic event is the Dongsha Events occurring between approximately 10.5–5.5 Ma BP (Wu et al., 2014a). Consequences of the Dongsha Events were generalized uplift of the northern continental slope of the SCS, the fault of the upper crust, erosion and widespread magma activities (Li et al., 2016).

Additionally, water circulations of the SCS comprise SCS surface water, SCS intermediate water, and SCS deep water (Wang and Li, 2009). The range of the surface water is commonly above 350 m-depth, while the lower limit of the Intermediate Water is still debated, with water depth of 1 000 m (Zhao et al., 2009), or 1 200 m (Li et al., 2013), or exceeding 1 500 m (Xie et al., 2013), and so on. Pathways for the surface water circulation are cyclonic in winter and anti-cyclonic in summer (Xu et al., 2014), whereas the intermediate water in the northern South China Sea should be anti-cyclonic (Li et al., 2013) (Fig. 1a). Unlike the surface and intermediate water, the SCS deep water was proven to be cyclonic (Gong et al., 2012) (Fig. 1a). The continental slope in the study area is mainly sculpted by the SCS intermediated water and deep water.

3 Data and methods

This study was based on numerous 2D seismic profiles provided by the Guangzhou Marine Geological Survey. These seismic profiles almost covered the whole study area, with water depth of approximately 500–3 100 m. The seismic data consist of NW–SE and NE–SW seismic profiles with a trace interval of 6 m, the vertical scale of 3.0 cm/s, and the horizontal scale of 40.17 traces/cm. The two-way time of these profiles was converted to depth using the velocity of 1 500 m/s for water column. By applying the polynomial interpolation method to the depth data extracted from these seismic profiles, bathymetric grids were constructed at a grid resolution of 100 m×100 m. Then seafloor gradients were created, and each bathymetric grid has associated values of depth and slope magnitude. Gradient data were binned into 50 m depth intervals, and the average gradient of each interval was calculated. Types of the slope morphology were distinguished according to the slope structures, further evidenced by the results of Kruskal-Wallis One Way ANOVA Testing and Pairwise Comparison with no priori assumptions for the seafloor gradients of the slope. Based on the interpretations of the seismic data, igneous bodies and associated sedimentations were described and analyzed by typical seismic facies. Special attention was paid to the relationship between igneous bodies and modern slope morphology, therefore, the effects of igneous bodies on modification of the continental slope were documented.

4 Slope morphology features

Figure 1b presents the overall slope morphology in the study area, on the basis of which three types of the continental slope could be distinguished directly according to slope structures: (1) Type 1, a rough and steep slope with multiple igneous bodies; (2) Type 2, a relatively smooth and gentle slope with single igneous body; (3) Type 3, a smooth and gentle slope without igneous bodies. Subsequently, the differences of modern slope morphologies among three types of the slope were determined, using the Kruskal-Wallis One Way ANOVA Testing and Pairwise Comparison with no priori assumptions, and found to be significantly different (p=0.000<0.05, as shown in Table 1 and Table 2).

The slope morphology of Type 1 is primarily characterized by numerous morphology anomalies caused by igneous bodies, which could be easily recognized on the typical depth profile (Fig. 2a, Type 1). Like Fig. 2b, a pictured here, a wider shaded region occurred above approximately 2 100 m depth, representing ±1 standard deviation around the average gradient value of every given 50 m depth interval, indicates that the slope gradients exhibit considerable variability, with the maximum average gradient of these given 50 m depth bins reaching up to 7.13° in water depth between 1 200 and 1 250 m.

Although morphology anomalies could also be distinguished (Fig. 2a), the slope morphology of Type 2 varies from the rough and steep slope surface in type1, which is relatively smooth and gentle merely with a wider shaded region at approximately 2 400–2 850 m water depth. The maximum average gradient of these given 50 m intervals reached 5.21° in water depth of 2 750–2 800 m (Fig. 2b).

The slope morphology of Type 3 is mainly characterized by its pattern of consistently gentle seafloor gradients over its entire depth range (Figs 2a and b). Changes in slope with depth are very subtle on this slope, and the highest average slope value of these given 50 m intervals is 4.71°, in water depth of about 1 350–1 450 m, where is located in the slope break. The majority of the slope gradients are lower than 2.5°. What was less visible then, characterizing this slope morphology is a relatively narrow shaded region, representing ±1 standard deviation around the average gradient of every given 50 m depth interval.

5 Igneous bodies and associated sedimentary features

Based on the interpretations of the seismic data, igneous bodies and associated sedimentary features are recognized on the seismic profiles. Effects of igneous bodies on modification of modern slope morphology will be made in the discussion section.

5.1 *Contourite deposits between the igneous bodies*

Numerous igneous bodies could be recognized on the seis-

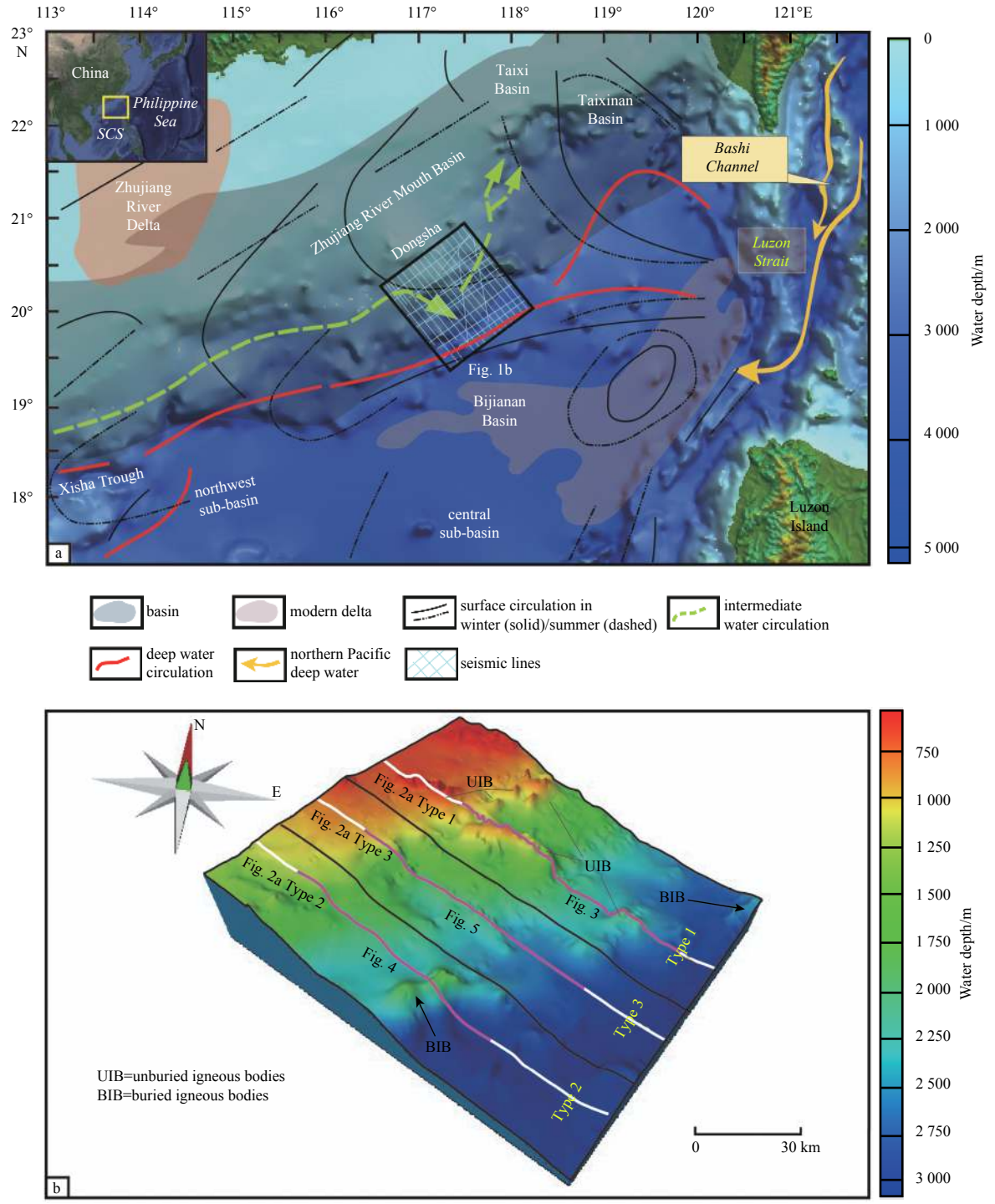

Fig. 1. Overview map of the mid-eastern part of the northern South China Sea and the study area. a. Global relief map of the mid-eastern part of the northern South China Sea, with the locations of the sedimentary basins, modern delta, and ocean current circulations (modified after Chen et al. (2014)); the yellow solid means that the northern Pacific deep water flows into the South China Sea via Bashi Channel and Luzon Strait (Gong et al., 2012); the red arrows are pathways for the circulation of the assumed deep water (modified after Chen et al. (2014)); the black dashed and solid arrows show the main surface circulation pathways in summer and winter, respectively (Wang and Li, 2009); boundary of the study area is shown in black rectangle; and the locations of seismic profiles are labeled by blue solid lines. b. Topographic map of the study area, presenting locations of the studied seismic lines in Figs 2–5, as well as different types of the continental slope in the study area.

mic profile apparently in Fig. 3, which show high amplitudes and chaotic reflections in the interior with a clear external outline, as well as numerous morphological highs on the seabed. However, these morphological highs may induce streamline distortions of oceanic currents, hence, affecting the sediment distribution around these morphological highs (Hernández-Molina et al.,

Table 1. Hypothesis test summary

Null hypothesis	Test	*P*	Decision
The distribution of gradient is the same across categories of Group	independent-samples Kruskal-Wallis Test	0	rejected the null hypothesis

Note: The significance level is 0.05.

Table 2. Pairwise comparison of three types of modern slope morphologies

Sample 1–Sample 2	Test statistics	Std. error	Std. test statistics	*P*
Type 2–Type 1	32 575.806	761.293	42.790	0
Type 2–Type 3	–48 530.480	728.965	–66.574	0
Type 1–Type 2	–15 954.674	699.463	–22.810	0

Note: The significance level is 0.05.

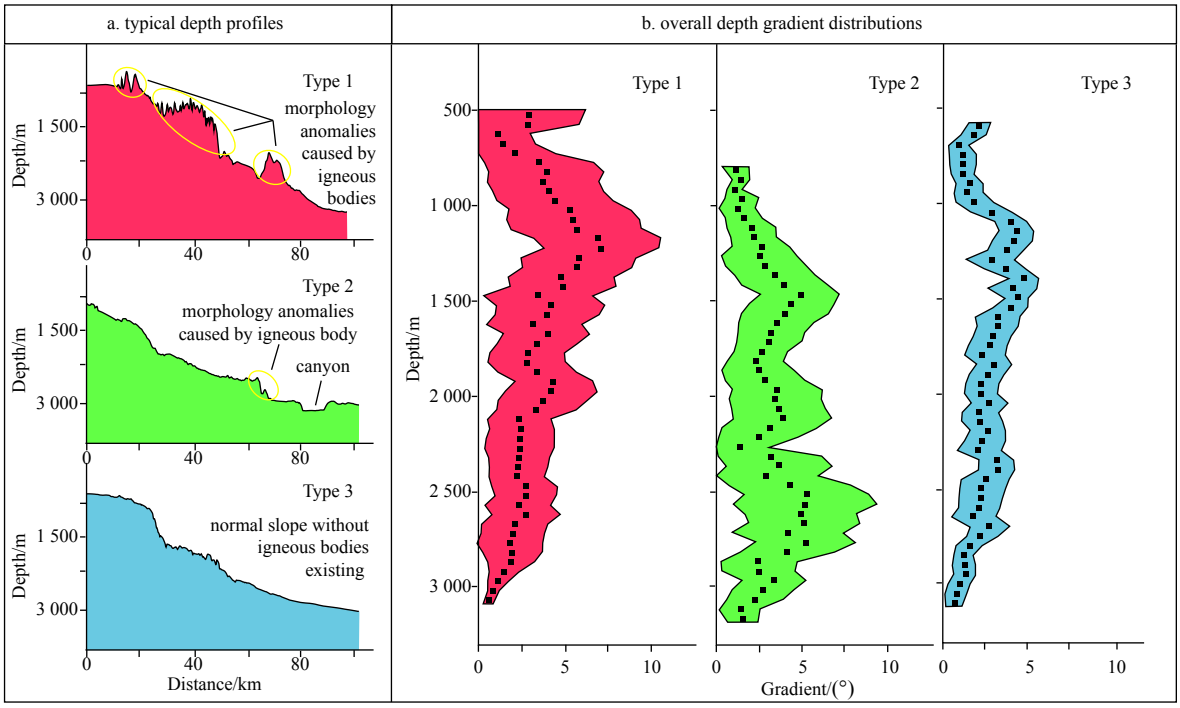

Fig. 2. Morphological characteristics of the modern slope in the study area. a. Typical depth profiles showing morphology anomalies of three types of the slope. b. Depth-gradient distributions, black dots indicate the average gradient of given 50 m depth bins, and the shaded region around black dots indicating ±1 standard deviation. Both Figs 2a and b are colored according to the results of Kruskal-Wallis One Way ANOVA Testing and Pairwise Comparison.

2006; Faugères and Stow, 2008; Chen et al., 2014). Different shear velocities are generated for diverse frictions when the bottom currents are deflected and intensified by morphological highs, formed by igneous bodies, and the Coriolis Force could push the bottom currents into the right in the northern hemisphere, as well as the degree of morphological convex results in a curved framework, where the secondary circulation occur (Faugères et al., 1999; Wynn and Stow, 2002; Li et al., 2013; Rebesco et al., 2014). Such as Fig. 3, the morphological depressions near these igneous bodies will be interpreted as moats. Both sides of the mounded-confined drifts are restricted by igneous bodies, and the mounded-confined drifts have the distinct bottom boundary with a relatively flat and smooth top. The bottom currents between these igneous bodies were intensified and deflected, hence, two deep and narrow moats were formed on both sides of the mounded-confined drifts. Nevertheless, the bottom currents near the rightness of the right igneous body on the section (Fig. 3), was not restricted, forming a relatively shallow and wide morphology depression also named moat, as well as the elongated-mounded drifts. The reflections of these drifts, in Fig. 3, show moderate to high amplitude and moderate to low continuity. The bottom currents away from the igneous bodies were not affected by the igneous bodies, which comprise the SCS intermediate and deep water, commonly formed sheeted drifts (Fig. 3).

5.2 *Slope block formed by the igneous body*

Equally, the single igneous body could also be determined by the seismic profile directly in Fig. 4, showing internal chaotic reflections with a clear external boundary. Near the abrupt morphology change on the left part of the section (Fig. 4), the slight depression will be interpreted as a moat. In Fig. 4, the rightness of the moat, a mounded topography could be observed, which could be interpreted as elongated-mounded drifts. This moat and drifts might be formed by the SCS deep water, which was deflected and intensified by the steeper slope morphology on the left side of the section (Fig. 4). Subsequently, destroyed by the

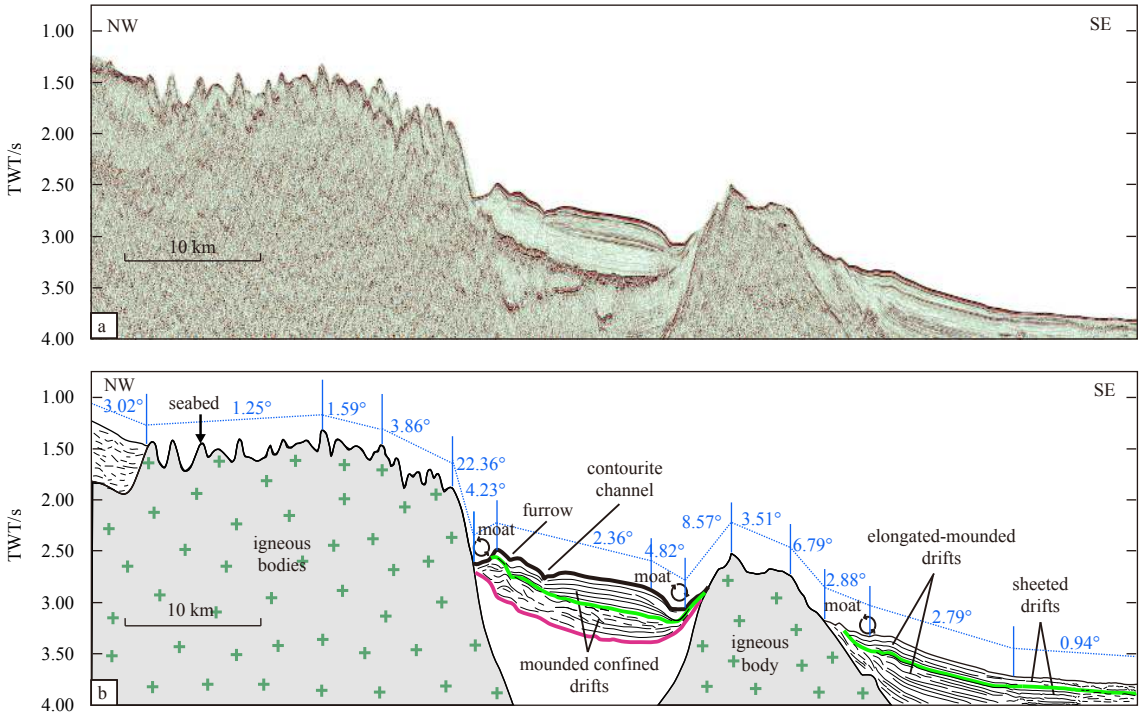

Fig. 3. NW-SE oriented profile (see the location in Fig. 1b). a. Original seismic profile. b. Interpreted profile showing the slope with multiple igneous bodies and its morphology changes; and the depressions formed by the igneous bodies could be filled with contourites (mounded confined drifts, elongated mounded drifts and sheeted drifts) at the meantime.

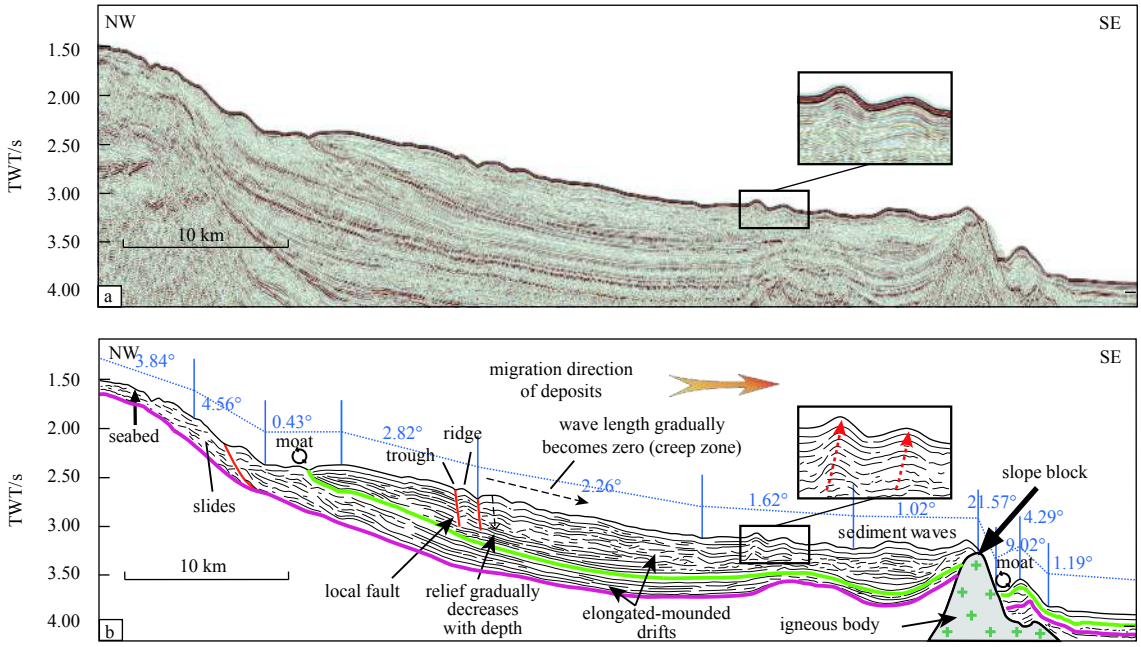

Fig. 4. NW-SE oriented profile (see the location in Fig. 1b). a. Original seismic profile. b. Interpreted profile displaying the slope with the single igneous body and its morphology changes; sediments were prevented by the igneous body from being transported downslope; and the inset showing sediment waves formed by the secondary circulation of bottom currents.

gravity force, a downslope creep zone was formed on the basis of the elongated-mounded drifts, with the presence of ridges, troughs, local faults and the gradually decreased wavelength and wave height. The downslope morphology anomalies caused by the igneous body on the seafloor, are still preserved well, whereas the upslope morphology anomalies had been eliminated by sediments. On the right side of the seismic profile in Fig. 4, the right-migrating sediment waves are presented. In fact, the migration directions of all deposits on the seismic profile trend parallel to the downslope direction. Moreover, it is clear that the igneous body, like a slope block, prevents the deposits from being transported into the abyssal plain. Above all, sediments could not be

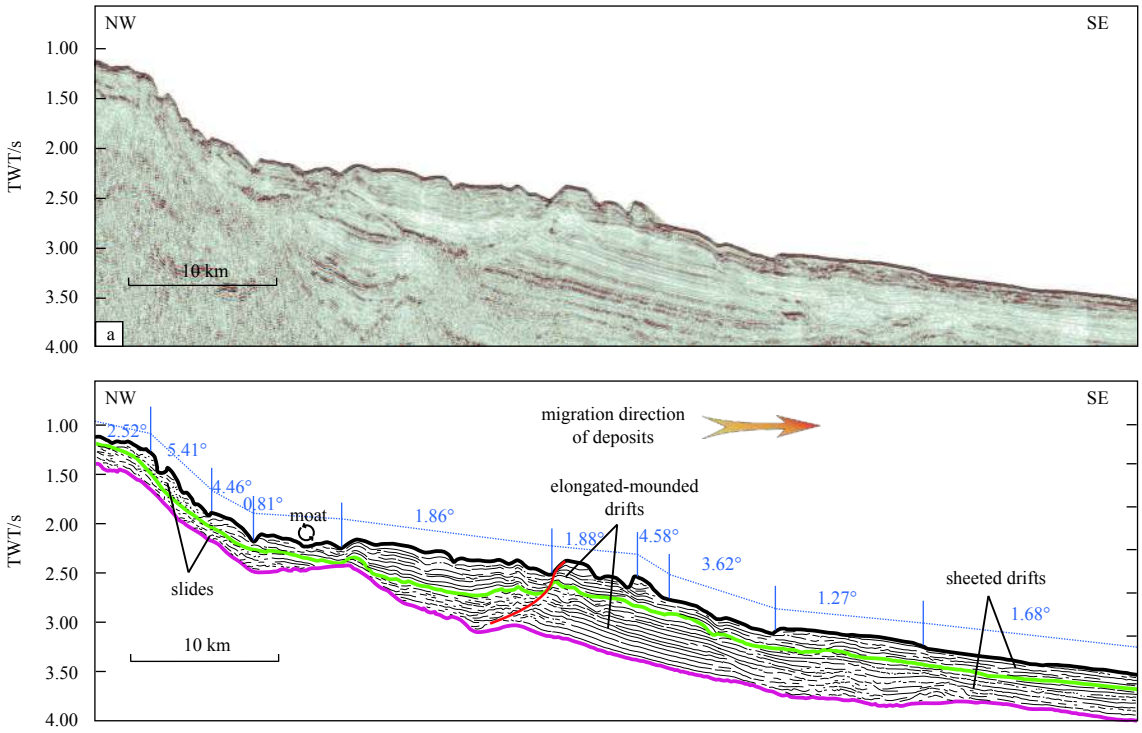

Fig. 5. NW-SE oriented profile (see the location in Fig. 1b). a. Original seismic profile. b. Interpreted profile exhibiting the slope without igneous body and its morphology changes; and sediments could be normally transported downslope by the secondary circulation of bottom currents.

transported into the abyssal plain until the upslope morphology anomalies caused by igneous body were eliminated by sediments.

6 Discussion

The continental slope in the study area has been subdivided into three types of the slope with different modern slope morphologies. The typical sedimentary features in Type 1 is represented by contourites related to igneous bodies and bottom currents (Fig. 3), while the sediments were prevented by the igneous body from being transported into the abyssal plain (Fig. 4) in Type 2. Unlike the sedimentary processes occurring in Types 1 and 2, sedimentary processes in Type 3 were not influenced by igneous bodies, just with normal clinoform progradation (Fig. 5). Previous studies attempting to study seismic patterns of most margins reveal that changes to the overall shape of a margin through time tend to be incremental, cumulative, and slow (Steckler et al., 1999; O'Grady et al., 2000). Equally, the distinctions among three types of modern slope morphologies will gradually decrease. Finally, they will be eliminated, therefore, the overall slope morphology becomes extremely smooth and gentle.

To better understand the effects of igneous bodies on modification of modern slope morphology in detail, conceptual models for three types of the slope explaining the effects of igneous bodies on controlling sedimentary processes, in the study area, were established and presented in Fig. 6.

On the slope with multiple igneous bodies (Fig. 6Aa), slope morphology anomalies were formed by the intercepts and complex shapes of igneous bodies firstly. Meanwhile, the presence of the igneous bodies separated the slope into two or more upper sub-sags and a lower main-sag, making streamline distortions of bottom currents to form contourites. These upper sub-sags and the lower main-sag could be filled simultaneously. First of all, the sedimentation unit 1will be formed (Step 1), followed by the sedimentation 2 (Step 2). At this point, slope morphology anomalies caused by multiple igneous bodies were eliminated completely. The sedimentation unit 3 (Step 3) represents normal sedimentation.

However, as shown in Fig. 6Ba, the single igneous body merely separated the slope into an upper sub-sag and a lower main-sag. On this slope, the migration direction of deposits is downslope, and the sediments could be transported by gravity flows or bottom currents. The sediments will be prevented by the igneous body from migrating into the main-sag until the sub-sag is filled up. Therefore, the sedimentation unit 1 will form at first, followed by the sedimentation unit 2, finally the sedimentation unit 3. In comparison, on the slope without igneous bodies, sedimentary processes were not affected by igneous bodies, with normal slope aggradations all the time (Fig. 6C).

In the study area, the slope with multiple igneous bodies (Type 1) is at the end of the Step 1 (Fig. 6Ab), while the slope with single igneous bodies (Type 2) is at the beginning of Step 2 (Fig. 6Bc), in which sediments start to be transported into the lower main-sag to form sedimentation unit 2. Although the modern slope morphologies of these slopes will constantly change over time due to the different Steps that they will be in, the morphology of the overall slope will tend to be smooth and gentle, therefore, the differences among three types of the modern slope morphologies will decrease constantly. Modern slope morphologies in the study area are the results of adjustments of the continental slope due to the intrusion of igneous bodies and associated sedimentary processes. The distinctions among three types of modern slope morphologies indicate different depositional conditions and adjustments of slope morphologies. Additionally, the distri-

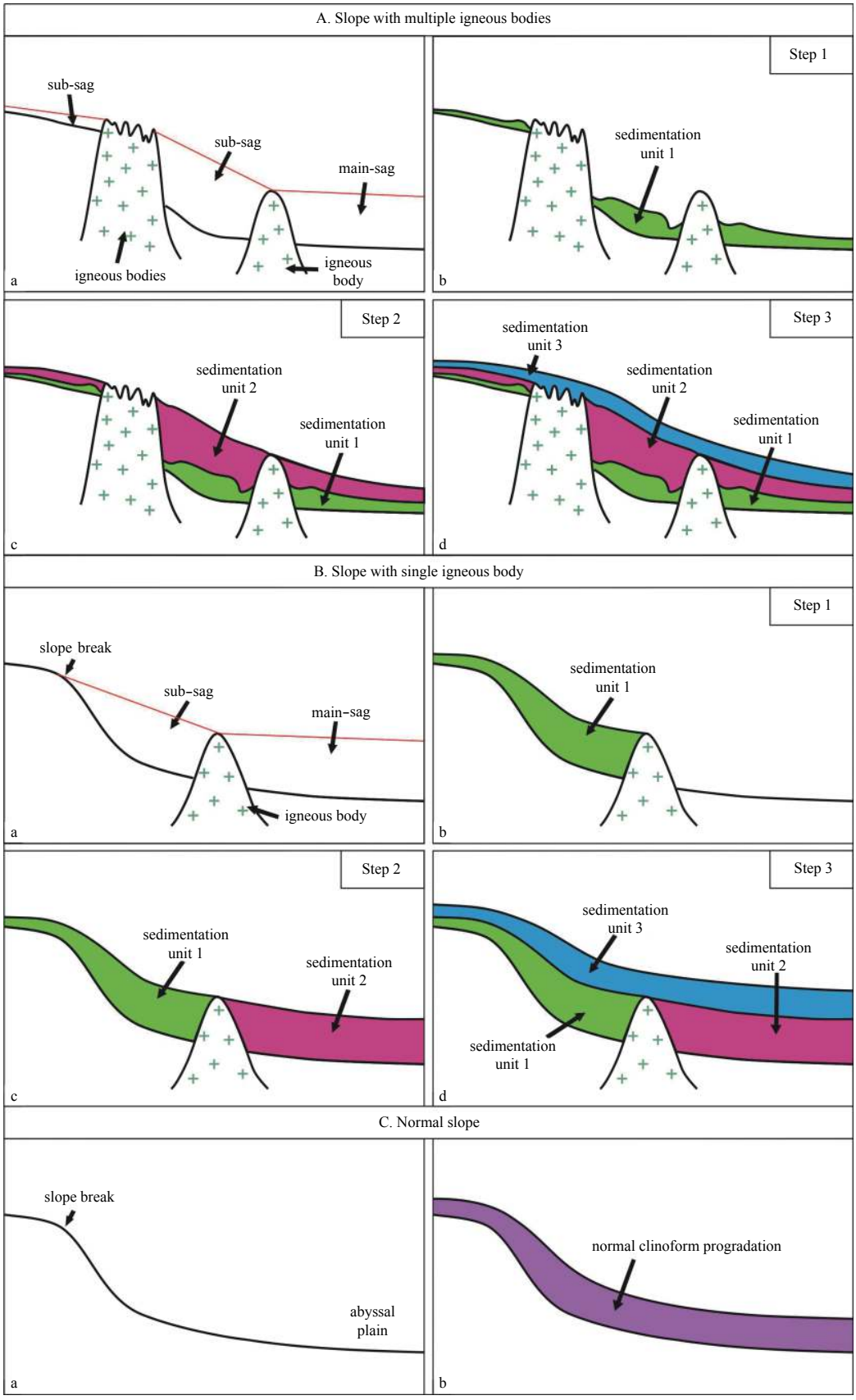

Fig. 6. Conceptual models for explaining the effects of igneous bodies on controlling sedimentary processes in the study area, which help us understand the different depositional conditions and different adjustments of slope morphologies mainly caused by igneous bodies.

butions of foot lines of the continental slope may change over time, due to the adjustment of slope morphologies (e.g., Wu et al., 2014b, 2017).

7 Conclusions

This paper has investigated a 2D multi-channel reflection seismic data, explaining the effects of igneous bodies on modification of modern slope morphology, offshore Dongsha Islands, South China Sea. The main conclusions of this study are as follows.

(1) The continental slope, in the study area, could be subdivided into three types according to slope structures, i.e., the rough and steep slope with multiple igneous bodies (Type 1), the relatively smooth and gentle slope with single igneous body (Type 2), and the smooth and gentle slope without igneous bodies (Type 3). Moreover, modern slope morphologies of three types of the slope reveal significant differences, evidenced by the results of Kruskal-Wallis One Way ANOVA Testing and Pair- wise Comparison.

(2) The igneous bodies in Type 1 separated the slope into two or more upper sub-sags and a lower main-sag, in which these upper sub-sags and the lower main-sag could be filled with sediments transported by alongslope bottom currents simultaneously. However, the single igneous body in Type 2 just separated the slope into an upper sub-sag and a lower main-sag, in which the sediments could be transported into the lower main-sag only after the upper sub-sag has been filled up. Type 3 represents a normal slope with common clinoform progradation.

(3) Due to the different steps that these slopes will be in, modern slope morphologies will constantly change over time. The distinctions among three types of modern slope morphologies indicate different depositional conditions and adjustments of slope morphologies.

Acknowledgements

We acknowledge the Guangzhou Marine Geological Survey for providing numerous 2D seismic profiles. We also express our appreciations for the help provided by colleagues of the Guangzhou Marine Geologic Survey and Key Laboratory of Tectonics and Petroleum Resources of Ministry of Education, China University of Geosciences.

References

Adams E W, Schlager W, Wattel E. 1998. Submarine slopes with an exponential curvature. Sedimentary Geology, 117(3–4): 135–141, doi: 10.1016/S0037-0738(98)00044-X

Brothers D S, Brink U S T, Andrews B D, et al. 2013. Geomorphic characterization of the U. S. Atlantic continental margin. Marine Geology, 338: 46–63

Cacchione D A, Pratson L F, Ogston A S. 2002. The shaping of continental slopes by internal tides. Science, 296(5568): 724–727, doi: 10.1126/science.1069803

Chen Hui, Xie Xinong, Van Rooij D, et al. 2014. Depositional characteristics and processes of alongslope currents related to a seamount on the northwestern margin of the Northwest Sub-Basin, South China Sea. Marine Geology, 355: 36–53, doi: 10.1016/j.margeo.2014.05.008

Cheng Shixiu, Li Sanzhong, Suo Yanhui, et al. 2012. Cenozoic tectonics and dynamics of basin groups of the northern South China Sea. Marine Geology & Quaternary Geology (in Chinese), 32(6): 79–93

Del Bianco F, Gasperini L, Angeletti L, et al. 2015. Stratigraphic architecture of the Montenegro/N. Albania continental margin (Adriatic sea-central Mediterranean). Marine Geology, 359: 61–74

Faugères J C, Stow D A V, Imbert P, et al. 1999. Seismic features diagnostic of contourite drifts. Marine Geology, 162(1): 1–38, doi: 10.1016/S0025-3227(99)00068-7

Faugères J C, Stow D A V. 2008. Contourite drifts: nature, evolution and controls. Developments in Sedimentology, 60: 257–288, doi: 10.1016/S0070-4571(08)10014-0

García M, Hernández-Molina F J, Llave E, et al. 2009. Contourite erosive features caused by the Mediterranean outflow water in the gulf of Cadiz: quaternary tectonic and oceanographic implications. Marine Geology, 257(1–4): 24–40, doi: 10.1016/j.margeo.2008.10.009

Goff J A. 2001. Quantitative classification of canyon systems on continental slopes and a possible relationship to slope curvature. Geophysical Research Letters, 28(23): 4359–4362, doi: 10.1029/2001GL013300

Gong Chenglin, Wang Yingmin, Peng Xuechao, et al. 2012. Sediment waves on the South China Sea slope off southwestern Taiwan: implications for the intrusion of the northern pacific deep water into the South China Sea. Marine and Petroleum Geology, 32(1): 95–109, doi: 10.1016/j.marpetgeo.2011.12.005

Hernández-Molina F J, Larter R D, Rebesco M, et al. 2006. Miocene reversal of bottom water flow along the Pacific Margin of the Antarctic Peninsula: stratigraphic evidence from a contourite sedimentary tail. Marine Geology, 228(1–4): 93–116, doi: 10.1016/j.margeo.2005.12.010

Kenyon P M, Turcotte D L. 1985. Morphology of a delta prograding by bulk sediment transport. GSA Bulletin, 96(11): 1457–1465, doi: 10.1130/0016-7606(1985)96<1457:MOADPB>2.0.CO;2

Li Wei, Alves T M, Wu Shiguo, et al. 2016. A giant, submarine creep zone as a precursor of large-scale slope instability offshore the Dongsha Islands (South China Sea). Earth and Planetary Science Letters, 451: 272–284, doi: 10.1016/j.epsl.2016.07.007

Li Pinglu, Rao Chuntao. 1994. Tectonic characteristics and evolution history of the Pearl river mouth basin. Tectonophysics, 235(1–2): 13–25, doi: 10.1016/0040-1951(94)90014-0

Li Hua, Wang Yingmin, Zhu Weilin, et al. 2013. Seismic characteristics and processes of the Plio-Quaternary unidirectionally migrating channels and contourites in the northern slope of the South China Sea. Marine and Petroleum Geology, 43: 370–380, doi: 10.1016/j.marpetgeo.2012.12.010

Lüdmann T, Wong H K. 1999. Neotectonic regime on the passive continental margin of the northern South China Sea. Tectonophysics, 311(1–4): 113–138, doi: 10.1016/S0040-1951(99)00155-9

O'Grady D B, Syvitski J P M, Pratson L F, et al. 2000. Categorizing the morphologic variability of siliciclastic passive continental margins. Geology, 28(3): 207–210, doi: 10.1130/0091-7613(2000)28<207:CTMVOS>2.0.CO;2

Pratson L F, Haxby W F. 1996. What is the slope of the U. S. continental slope?. Geology, 24(1): 3–6, doi: 10.1130/0091-7613(1996)024<0003:WITSOT>2.3.CO;2

Rebesco M, Hernández-Molina F J, Van Rooij D, et al. 2014. Contourites and associated sediments controlled by deep-water circulation processes: state-of-the-art and future considerations. Marine Geology, 352: 111–154, doi: 10.1016/j.margeo.2014.03.011

Sayago-Gil M, Long D, Hitchen K, et al. 2010. Evidence for current-controlled morphology along the western slope of Hatton Bank (Rockall Plateau, NE Atlantic Ocean). Geo-Marine Letters, 30(2): 99–111, doi: 10.1007/s00367-009-0163-5

Schlager W, Camber O. 1986. Submarine slope angles, drowning unconformities, and self-erosion of limestone escarpments. Geology, 14(9): 762–765, doi: 10.1130/0091-7613(1986)14<762:SSADUA>2.0.CO;2

Song Xiaoxiao, Li Chunfeng, Yao Yongjian, et al. 2017. Magmatism in the evolution of the South China Sea: geophysical characterization. Marine Geology, 394: 4–15, doi: 10.1016/j.margeo.2017.07.021

Steckler M S, Mountain G S, Miller K G, et al. 1999. Reconstruction of Tertiary progradation and clinoform development on the New Jersey passive margin by 2-D backstripping. Marine Geology, 154(1–4): 399–420, doi: 10.1016/S0025-3227(98)00126-1

Taylor B, Hayes D E. 1983. Origin and history of the South China Sea basin. In: Hayes D E, ed. The Tectonic and Geologic Evolution

of Southeast Asian Seas and Islands: Part 2. Washington, DC: AGU Geophysical Monograph, 23–56

Wang Pinxian, Li Qianyu. 2009. Oceanographical and geological background. In: Wang Pinxia, Li Qianyu, eds. The South China Sea: Paleoceanography and Sedimentology. Dordrecht: Springer

Wu Shiguo, Gao Jinwei, Zhao Shujuan, et al. 2014a. Post-rift uplift and focused fluid flow in the passive margin of northern South China Sea. Tectonophysics, 615–616: 27–39, doi: 10.1016/j.tecto.2013.12.013

Wu Ziyin, Li Jiabiao, Li Shoujun, et al. 2017. A new method to identify the foot of continental slope based on an integrated profile analysis. Marine Geophysical Research, 38(1–2): 199–207, doi: 10.1007/s11001-016-9273-4

Wu Ziyin, Li Jiabiao, Jin Xianglong, et al. 2014b. Distribution, features, and influence factors of the submarine topographic boundaries of the Okinawa trough. Science China Earth Sciences, 57(8): 1885–1896, doi: 10.1007/s11430-013-4810-3

Wynn R B, Stow D A V. 2002. Classification and characterisation of deep-water sediment waves. Marine Geology, 192(1–3): 7–22, doi: 10.1016/S0025-3227(02)00547-9

Xie Qiang, Xiao Jingen, Wang Dongxiao, et al. 2013. Analysis of deep-layer and bottom circulations in the South China Sea based on eight quasi-global ocean model outputs. Chinese Science Bulletin, 58(32): 4000–4011, doi: 10.1007/s11434-013-5791-5

Xu Weihai, Yan Wen, Chen Zhong, et al. 2014. Organic matters and lipid biomarkers in surface sediments from the northern South China Sea: origins and transport. Journal of Earth Science, 25(1): 189–196, doi: 10.1007/s12583-014-0412-z

Yao Bochu, Wan Ling, Wu Nengyou. 2004. Cenozoic plate tectonic activities in the Great South China Sea area. Geology in China (in Chinese), 31(2): 113–122

Zhang Liansheng, Zhong Dalai. 1996. The red river strike-slip shear zone and Cenozoic tectonics of east Asia continent. Scientia Geologica Sinica (in Chinese), 31(4): 327–341

Zhao Quanhong, Li Qianyu, Jian Zhimin. 2009. Deep waters and oceanic connection. In: Wang Pinxian, Li Qianyu, eds. The South China Sea. Dordrecht: Springer, 395–437